

# Formulation and Optimization of Valganciclovir-loaded Nanosponges

Alka Singh\*, Chetan S Chauhan

*Bhupal Nobles' Institute of Pharmaceutical Sciences, Bhupal Nobles' University, Udaipur, Rajasthan, India.*

*Received: 03<sup>rd</sup> November, 2023; Revised: 16<sup>th</sup> December, 2023; Accepted: 18<sup>th</sup> February, 2024; Available Online: 25<sup>th</sup> March, 2024*

## ABSTRACT

The objective of our study was to form a novel method of delivering drugs that would improve the effectiveness of valganciclovir, an antiviral medication used to treat cytomegalovirus (CMV) infection in individuals with weakened immune systems. The drug's induction dosage has limited penetration and requires very high doses. The nanosponges were synthesized using the emulsion solvent diffusion method, employing a 3<sup>2</sup> full factorial design to determine the combined impact of 2 independent variables: Quantity of ethyl cellulose and stirring speed. The dependent variables assessed were zeta potential, polydispersity index (PDI), and entrapment efficiency. Improved formulation exhibited an entrapment efficiency of 83.61%, a zeta potential of -17.6 mV, and a PDI of 0.51. The improved formulation exhibited a continuous and controlled release of the medication. The produced nanosponges were characterized using fourier transform infrared (FTIR), differential scanning calorimetry (DSC), and scanning electron microscopy (SEM).

**Keywords:** Nanosponges, Valganciclovir, 3<sup>2</sup> full factorial design, Emulsion solvent diffusion.

International Journal of Drug Delivery Technology (2024); DOI: 10.25258/ijddt.14.1.01

**How to cite this article:** Singh A, Chauhan CS. Formulation and Optimization of Valganciclovir-loaded Nanosponges. International Journal of Drug Delivery Technology. 2024;14(1):1-8.

**Source of support:** Nil.

**Conflict of interest:** None

## INTRODUCTION

Cytomegalovirus (CMV) is a herpesvirus that can infect immunocompromised people. It is the most common and prominent cause of death in people suffering from human immunodeficiency virus (HIV) / Acquired immunodeficiency syndrome (AIDS). It can manifest clinically in several ways, such as encephalitis, retinitis, colitis, pneumonitis, and esophagitis. CMV infection treatment depends on the severity of the condition and the specific population affected.<sup>1-2</sup>

Valganciclovir (VGC) is a biopharmaceutics classification system (BCS) class III drug that is freely soluble and poorly permeable. The low permeability is the rate-limiting factor for its bioavailability. Valganciclovir is often administered orally as a prodrug that is converted to the active form, ganciclovir, in the body to improve its bioavailability. Ganciclovir, the active metabolite of valganciclovir, is also a BCS class III drug. It is utilized for the treatment of certain viral infections, especially those caused by CMV.<sup>3</sup> The induction dose of VGC is 900 mg *b.d.* followed by a maintenance dose 900 mg, which is very high and leads to a number of side effects like bone marrow suppression, severe gastrointestinal symptoms (e.g., persistent vomiting, severe diarrhea), etc.<sup>4</sup> The present study aimed to develop nanosponges (NS) a nano-carrier that can decrease the dosage and side effects related to dose by sustaining the release of the drug.

Nanosponges (NS) are minuscule sponges, comparable in size to a virus, that enclose cavities filled with various

medications. These sponges go throughout the body until they locate where they need to attach, and then they slowly release the medicine.<sup>5</sup> They exhibit a five-fold increase in efficiency compared to conventional methods in administering medications for breast cancer while also being devoid of irritant, mutagenic, allergenic, and poisonous properties. Nanosponges (NS) have a solid structure and have the ability to transport both lipophilic (fat-loving) and hydrophilic (water-loving) compounds. Additionally, they aid in enhancing the solubility of molecules that are less soluble or poorly soluble in water.<sup>6,7</sup> These substances have a porous structure, are not harmful to health, do not dissolve in water or other organic solvents, and remain stable at temperatures up to 300°C. The research involved the development of VGC-loaded NS using a 3<sup>2</sup>-complete factorial model and an improved formulation.

## MATERIALS AND METHODS

### Materials

VGC was acquired as a complimentary sample from Aurobindo Pharma Limited in Hyderabad, India. Dichloromethane (DCM), polyvinyl alcohol (PVA), and ethyl cellulose (EC), were procured from Loba Chemie. All compounds utilized in the investigation were of analytical grade.

### Experimental Design

The present investigation utilized a 3<sup>2</sup> complete factorial design. The design considered two factors, which were assessed

\*Author for Correspondence: [alkasingh1790@gmail.com](mailto:alkasingh1790@gmail.com)

**Table 1:** 3<sup>2</sup> Full factorial design and levels

Independent variables	Levels		
	-1	0	1
X1 (VGC: EC, w/w)	1:2	1:4	1:6
X2 (Stirring speed, rpm)	1000	1500	2000

at 3 levels: high (1), medium (0), and low (-1). Independent variables chosen were EC ratio (X1) and stirring speed (X2) impacts of the VGC medication. The dependent variables chosen were the polydispersity index (Y1), zeta potential (Y2), as well as entrapment efficiency (Y3). Table 1 displays the levels and factors of the factorial design.<sup>8</sup>

### Formulation of VGC-loaded NS

VGC NS were prepared by the emulsion solvent diffusion method. VGCV as well as EC were dissolved in DCM to obtain phase 1. Phase 2 was prepared adding PVA to distilled water. Both phases were kept separately on a magnetic stirrer for 10 minutes. Phase 1 was added slowly to phase 2 with continuous stirring at room temperature. The mixture was then homogenized at different stirring speeds as given in Table 2 for two hours. After this step, the prepared nanosponges were filtered and dried in a vacuum oven at 40°C for 12 hours.<sup>9-12</sup> All nine formulation batches are represented in Table 2.

### Characterization of Valganciclovir-loaded Nanosponges

#### Percentage yield

The percentage yield of several batches of NS was determined by applying the following formula, which involved utilizing the weight of the finished product after drying [practical mass] in relation to original total weight of medication as well as the polymer that was utilized for the creation of NS [theoretical mass]:

$$\text{Percentage yield} = (\text{Practical mass/theoretical mass}) \times 100$$

#### Particle size, polydispersity index, zeta potential

Polydispersity index (PDI) as well as mean particle size were found utilizing dynamic light scattering (Worcestershire, Malvern Zetasizer Nano, UK) at a fixed scattering angle of 90°. Following appropriate dilution with milli-Q water, all samples underwent room temperature analysis. With an extra electrode inserted inside the zeta sizer, the zeta potential of each sample

was determined using the same device. The measurements were all made three times.<sup>13</sup>

#### Entrapment efficiency

The weighed quantity of VGC-loaded NS (10 mg) was dissolved in methanol and sonicated to break the complex. The centrifuged, filtered supernatant was then appropriately diluted and subjected to ultraviolet spectrophotometer analysis at  $\lambda_{\text{max}}$  251 nm. The below-given formula calculated entrapment efficiency:

$$\text{Entrapment efficiency} = (\text{Entrapped drug concentration} / \text{Theoretical drug concentration}) \times 100$$

#### Surface morphology

The scanning electron microscopy (SEM) technique was utilized to investigate the VGC-loaded NS's surface morphology. Following the application of a concentrated aqueous suspension to a slab, the slab was subsequently subjected to vacuum drying. The sample was then placed in a cathodic evaporator and covered with a coating of gold twenty nanometers thick. An image processing program was used to enhance the photographs, and the individual drug and NS diameters were measured to get the mean particle size.<sup>14</sup>

#### Fourier transform infrared spectroscopy

Fourier transform infrared (FTIR) spectra were recorded on FTIR spectrophotometer to study any interaction between VGC and excipients. FTIR of valganciclovir, their physical mixture and NS were observed. A potassium bromide pellet method was adopted for the detection of the functional group of the drug by FTIR analysis. FTIR spectra of the VGC, excipients and formulated NS were noted between 400 to 4000 cm<sup>-1</sup>.<sup>15,16</sup>

#### Differential scanning calorimetry analysis

Shimadzu Corporation's DSC-60 Plus was used to study the thermal behavior of the formulation and drug. The weighed amount of samples were sealed and heated from 0 to 300°C at a rate of 10°C/min while being purged with nitrogen at a flow rate of 10 mL/min and a thermogram was recorded.<sup>17</sup>

#### In-vitro drug release

For the purpose of analyzing the patterns of drug release, dissolution experiments were carried out with the assistance of a dialysis membrane. The hydrophilic dialysis membrane (110) performs the function of a divider between the two

**Table 2:** Valganciclovir loaded nanosponges formulations

Formulation	VGCV: EC (w/w)	PVA (%w/v)	DCM (mL)	Stirring rate (rpm)	Stirring time (H)	Water (mL)
F1	1:2	1	10	1000	2	20
F2	1:2	1	10	1500	2	20
F3	1:2	1	10	2000	2	20
F4	1:4	1	10	1000	2	20
F5	1:4	1	10	1500	2	20
F6	1:4	1	10	2000	2	20
F7	1:6	1	10	1000	2	20
F8	1:6	1	10	1500	2	20
F9	1:6	1	10	2000	2	20

**Table 3:** Percentage yield of valganciclovir-loaded formulations

Formulation	Percentage yield (%)			Average ± Standard deviation
	1	2	3	
F1	67.28	65.34	68.51	67.04 ± 1.60
F2	58.9	61.67	55.96	58.84 ± 2.86
F3	65	62.73	60.45	62.73 ± 2.28
F4	52.5	49.58	47.33	49.80 ± 2.59
F5	68	64.62	67.91	66.84 ± 1.93
F6	70.8	67.95	71.79	70.18 ± 1.99
F7	76	74.31	70.62	73.64 ± 2.75
F8	78.2	76.62	73.61	76.14 ± 2.33
F9	41.76	38.24	41.39	40.46 ± 1.93

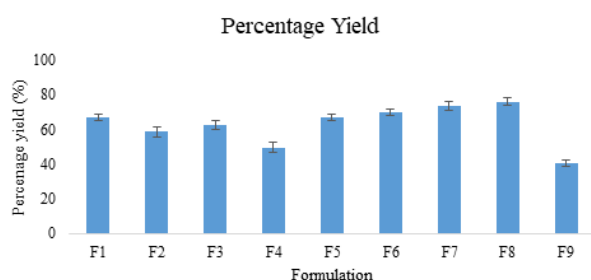


**Figure 1:** %yield of various batches of VGC-loaded NS

compartments. An experiment was conducted in 0.1N hydrochloric acid and 7.4 phosphate buffer solution at 37°C, stirring at 50 rpm. On a regular basis, the sample aliquots were removed at intervals that had been previously set, and they were thereafter replaced with an equivalent volume of new medium. In addition, to ascertain the percentage of cumulative drug release data recorded throughout the required time period, the collected samples were filtered, correctly diluted, and examined at a wavelength of 251 nm.<sup>18,19</sup>

**RESULTS AND DISCUSSIONS**

**Percentage Yield**

The percentage yield is represented in Table 3. The %yield of the prepared NS was found to be between 40 to 76%. Formulation F8 exhibited the maximum percentage yield (76.14% ± 2.33), while F9 exhibited the minimum percentage yield (40.46% ± 1.93). The results of percentage yield studies are shown below in the form of a graph, along with error bars in Figure 1.

**Statistical Analysis**

The present investigation utilized a 3<sup>2</sup> complete factorial design. The concept involved the evaluation of two elements at three levels: high (1), medium (0), and low (-1). Independent variables selected for analysis were the VGC (drug) : EC ratio (X1) in addition to stirring speed (X2) effects. The dependent variables chosen were the polydispersity index (Y1), zeta potential (Y2), and entrapment efficiency (Y3). Table 4 displays the levels and factors of the factorial design.<sup>8</sup>

$$Y = b_0 + b_1X_1 + b_2X_2 + b_{12}X_1X_2 + b_{11}X_1^2 + b_{22}X_2^2$$

The dependent variable, Y, is represented by an arithmetic mean of 9 runs, b<sub>0</sub>. The estimated coefficient for factor X<sub>1</sub> is denoted as b<sub>1</sub>. The primary impacts (X<sub>1</sub> as well as X<sub>2</sub>) indicate the average outcome of altering one element individually from its minimum to maximum value. In statistical analysis, the interaction terms, denoted as X<sub>1</sub>X<sub>2</sub>, quantify the effect of changing 2 factors simultaneously on the response variable. Variables X<sub>1</sub><sup>2</sup> and X<sub>2</sub><sup>2</sup> are employed for the analysis of nonlinearity. The PDI, zeta potential, and entrapment efficiency exhibited significant variability across all nine batches, ranging from F1 to F9 as shown in Table 4. The analysis of the data demonstrated a significant correlation between the chosen independent variables and the PDI, zeta potential, and entrapment efficiency values. The equations that have been adjusted to represent the response factors can be found in Table 5. Using polynomial equations, one can arrive at conclusions by considering the coefficient’s magnitude and mathematical sign of the coefficient, which can be either +ve or -ve. Table 6 displays the outcome of ANOVA, or analysis of variance, conducted to find relevant components.

The strong correlations between PDI, zeta potential, and entrapment efficiency (Table 6) show an excellent fit. The equation can be used to estimate the responses as a minor error of variance was shown in replicates.

**Polydispersity Index**

A significance level of coefficient b<sub>22</sub> and b<sub>12</sub> was found to be P = 0.95362 and P = 0.6395, respectively, which was greater than p < 0.05 and hence insignificant for determination of polydispersity and particle size of NS formulation and therefore omitted from the full model. Coefficient b1, b2, b11 were found significant at p < 0.05 and used for concluding contour plots. The results of the model’s testing in sections are presented in Table 6.

After analyzing the contour plot and surface response plot given in Figures 2 and 3, it was concluded that the PDI of VGC-loaded NS ranges between 0.06 to 0.604, which is less than 1.0

## Formulation of Valganciclovir-loaded Nanosponges

**Table 4:** Factorial layout and responses of valganciclovir loaded nanosponges

Batch code	Variable levels in coded form		$Y_1$ (PDI)	$Y_2$ (Zeta Potential)	$Y_3$ (Entrapment efficiency)
	$X_1$ (mg)	$X_2$ (rpm)			
F1	-1	-1	0.06	-10.9	54.02
F2	-1	0	0.16	-11.1	59.88
F3	-1	1	0.162	-12.1	63.99
F4	0	-1	0.202	-12.6	64.01
F5	0	0	0.225	-13	69.45
F6	0	1	0.299	-15.9	71.01
F7	1	-1	0.471	-15.4	77.51
F8	1	0	0.51	-17.6	83.61
F9	1	1	0.604	-20.8	82.32

**Table 5:** Summary of outcomes of regression analysis

For polydispersity index						
Response (PDI)	$b_0$	$b_1$	$b_2$	$b_{11}$	$b_{22}$	$b_{12}$
	0.24111	0.2005	0.0553	0.08583	0.00133	0.0077
For zeta potential						
response (Zeta)	$b_0$	$b_1$	$b_2$	$b_{11}$	$b_{22}$	$b_{12}$
	-13.3556	-3.28333	-1.65	-0.81667	-0.71667	-1.05
For entrapment efficiency						
response (Entrapment efficiency)	$b_0$	$b_1$	$b_2$	$b_{11}$	$b_{22}$	$b_{12}$
	69.60333	10.925	3.63	2.065	-2.17	-1.29

**Table 6:** Calculations for testing models in portions

For polydispersity index					
	DF	SS	MS	F	
Regression	5	0.2745	0.05491	61.5846	0.9903
For zeta potential					
	DF	SS	MS	F	
Regression	5	87.7877	17.5575	183.0324	0.9967
For entrapment efficiency					
	DF	SS	MS	F	
Regression	5	819.7978	163.9596	178.5792	0.9966

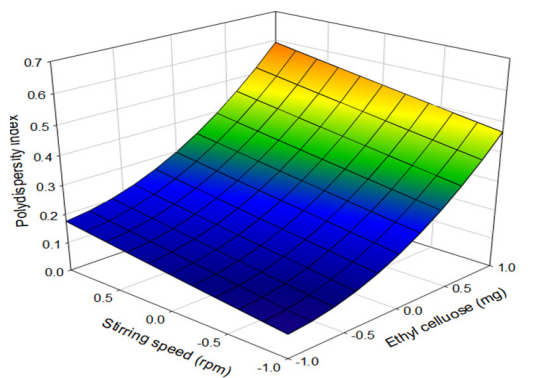


**Figure 2:** Valganciclovir: Ethyl cellulose ( $X_1$ ) and stirring speed ( $X_2$ ) effects on prepared nanosponges and polydispersity index ( $Y_1$ ) response surface plot

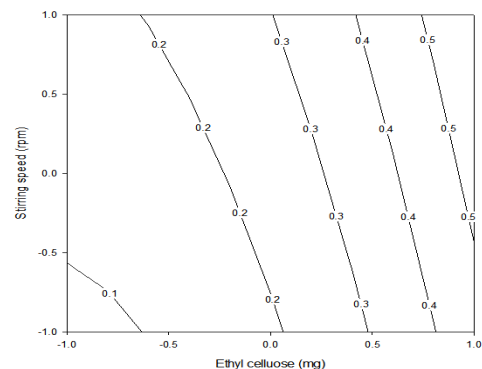


**Figure 3:** Valganciclovir: Ethyl cellulose ( $X_1$ ) and stirring speed ( $X_2$ ) effects on prepared nanosponges and polydispersity index ( $Y_1$ ) contour surface plot

and represents a narrower and uniform size distribution of the prepared formulation.

### Zeta Potential

Table 5 displays the outcomes of the statistical analysis. Based on the provided data, coefficients  $b_0$ ,  $b_1$ ,  $b_2$ ,  $b_{11}$ ,  $b_{22}$ , and  $b_{12}$  were determined to be statistically substantial at a significance level of  $p < 0.05$ . The outcomes of conducting the model testing in segments are depicted in Table 6.

An increase in ethyl cellulose concentration and stirring rate increases the colloidal stability of nanosponges formulation. It's important to note that the specific effects of zeta potential can depend on the composition of the particles,

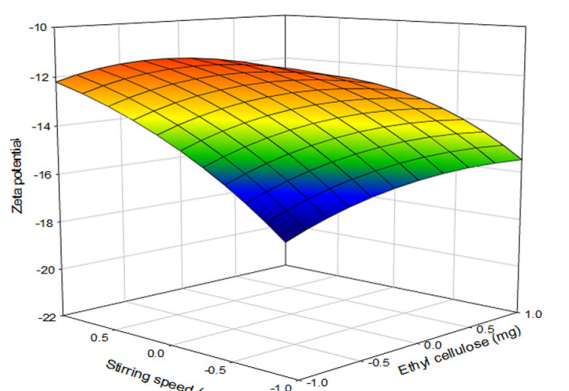


**Figure 4:** Valganciclovir: Ethyl cellulose (X1) as well as stirring speed (X2) effects on zeta potential (Y2) response surface plot

the surrounding medium, and the intended application. While a negative zeta potential often contributes to colloidal stability, the ideal zeta potential can vary based on the nanosponges' particular characteristics and the intended use requirements. A slightly negative zeta potential (between -10--30 mV) may be preferable. This is because a negative zeta potential can help minimize non-specific interactions with positively charged cell membranes.

Analyzing the contour plot shown in Figures 4 and 5 reveals that the whole contour plot has acceptable zeta values ranging between -10 and -21 mV.

### Entrapment Efficiency

The coefficients b11 and b12 were determined to have significance levels of  $p = 0.0555$  and  $p = 0.0742$ , respectively, indicating that they are not statistically significant and were therefore excluded from the model. Table 5 displays the outcomes of the statistical analysis. Coefficients b1, b2, and b22 were determined to be statistically substantial at a significance level of  $p < 0.05$ , hence were included in the model. The outcomes of evaluating the model in segments are illustrated in Table 6. The variables X1 (drug-to-polymer ratio) and X2 (stirring speed) are simultaneously manipulated to investigate potential interactions between the variables and their collective influence on entrapment efficiency. The contour plot analysis depicted in Figures 6 and 7 indicates that the entrapment efficiency of the manufactured nanosponges of VGCV varies between 54.02 and 83.61%.

The entrapment efficiency of nanosponges refers to the percentage of the encapsulated substance within the nanosponge formulation relative to the total amount of that substance used in the formulation. It is an important parameter that reflects the effectiveness of the nanosponge in ensnaring the desired payload.

### Surface Morphology

The SEM image of F8 formulation of VGC-loaded NS is given in Figure 8. The image reveals the porous, spherical nature of prepared NS. SEM images also confirm the nanoscopic range of the optimized formulation.

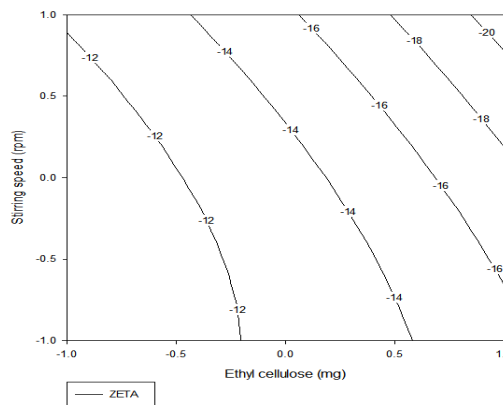


**Figure 5:** Valganciclovir: Ethyl cellulose (X1) as well as stirring speed (X2) effects on prepared nanosponges and zeta potential (Y2) contour surface plot

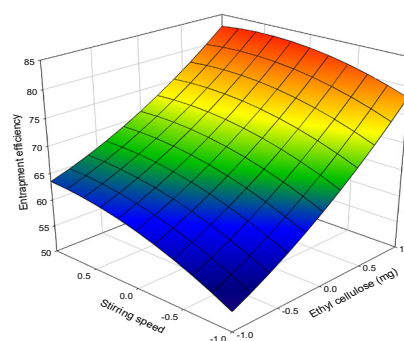


**Figure 6:** Valganciclovir: Ethyl cellulose (X1) and stirring speed (X2) effects on entrapment efficiency (Y3) response surface plot

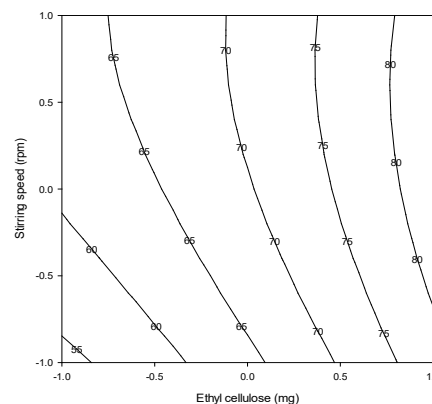


**Figure 7:** Valganciclovir: Ethyl cellulose (X1) and stirring speed (X2) effects on prepared nanosponges and entrapment efficiency (Y3) contour surface plot

### FTIR Spectroscopy

The spectra of optimized formulation F8 depict the characteristic peaks of valganciclovir at 2977.03 and 2877.23  $\text{cm}^{-1}$  for aromatic C-H stretching, a new peak occurred at 1982.73  $\text{cm}^{-1}$  which might be due of C=C stretching, as shown in Figures 9 (a) and (b). The other peaks when compared with the FTIR spectra of valganciclovir, showed no changes in peaks of aldehyde and aromatic groups at 1748.57  $\text{cm}^{-1}$  and 1695.95  $\text{cm}^{-1}$ , respectively.

## Formulation of Valganciclovir-loaded Nanosponges

**Table 7:** Dissolution study of pure drug (Valganciclovir)

Medium	Time (hours)	Percentage drug release (%)			Average $\pm$ SD
		1	2	3	
pH 1.2 HCl	0.5	13.95	13.32	14.55	13.94 $\pm$ 0.614
pH 1.2 HCl	1	15.14	14.68	16.84	15.55 $\pm$ 1.137
pH 1.2 HCl	1.5	16.80	16.56	22.63	18.67 $\pm$ 3.437
pH 1.2 HCl	2	18.87	18.31	19.26	18.81 $\pm$ 0.479
pH 7.4 Phosphate Buffer	3	11.59	12.48	12.12	12.06 $\pm$ 0.451
pH 7.4 Phosphate Buffer	4	12.20	13.65	13.04	12.96 $\pm$ 0.731
pH 7.4 Phosphate Buffer	6	13.42	15.65	14.80	14.62 $\pm$ 1.122
pH 7.4 Phosphate Buffer	8	14.43	17.05	16.43	15.97 $\pm$ 1.367
pH 7.4 Phosphate Buffer	10	16.27	18.81	17.89	17.66 $\pm$ 1.290
pH 7.4 Phosphate Buffer	12	18.04	20.21	19.97	19.41 $\pm$ 1.187
pH 7.4 Phosphate Buffer	14	20.04	21.90	21.90	21.28 $\pm$ 1.071
pH 7.4 Phosphate Buffer	16	23.34	23.14	23.67	23.39 $\pm$ 0.268
pH 7.4 Phosphate Buffer	18	25.29	26.04	26.21	25.85 $\pm$ 0.488
pH 7.4 Phosphate Buffer	20	28.43	27.92	27.92	28.09 $\pm$ 0.296
pH 7.4 Phosphate Buffer	22	31.90	29.99	30.22	30.70 $\pm$ 1.039
pH 7.4 Phosphate Buffer	24	34.08	32.53	32.84	33.15 $\pm$ 0.821
pH 7.4 Phosphate Buffer	26	37.68	33.87	35.39	35.64 $\pm$ 1.920
pH 7.4 Phosphate Buffer	28	38.20	36.01	36.57	36.93 $\pm$ 1.139
pH 7.4 Phosphate Buffer	30	38.74	37.87	38.11	38.24 $\pm$ 0.452

**Table 8:** Drug release of optimised F8 formulation

Medium	Time (hours)	Percentage drug release (%)			Average $\pm$ SD
		1	2	3	
pH 1.2 HCl	0.5	11.23	10.95	11.50	11.23 $\pm$ 0.273
pH 1.2 HCl	1	12.50	12.22	12.73	12.48 $\pm$ 0.256
pH 1.2 HCl	1.5	15.04	14.71	15.46	15.07 $\pm$ 0.377
pH 1.2 HCl	2	17.82	17.44	18.10	17.79 $\pm$ 0.333
pH 7.4 Phosphate Buffer	3	21.02	20.56	21.48	21.02 $\pm$ 0.460
pH 7.4 Phosphate Buffer	4	26.16	25.69	26.47	26.10 $\pm$ 0.390
pH 7.4 Phosphate Buffer	6	32.31	32.00	32.84	32.38 $\pm$ 0.428
pH 7.4 Phosphate Buffer	8	40.52	39.99	40.91	40.47 $\pm$ 0.464
pH 7.4 Phosphate Buffer	10	45.37	45.06	46.21	45.55 $\pm$ 0.596
pH 7.4 Phosphate Buffer	12	53.33	52.95	54.03	53.44 $\pm$ 0.548
pH 7.4 Phosphate Buffer	14	55.91	55.45	56.68	56.01 $\pm$ 0.622
pH 7.4 Phosphate Buffer	16	57.02	56.40	57.86	57.09 $\pm$ 0.734
pH 7.4 Phosphate Buffer	18	63.02	62.17	63.79	62.99 $\pm$ 0.809
pH 7.4 Phosphate Buffer	20	69.72	69.17	70.18	69.69 $\pm$ 0.508
pH 7.4 Phosphate Buffer	22	70.75	70.36	71.75	70.95 $\pm$ 0.712
pH 7.4 Phosphate Buffer	24	72.06	71.67	72.45	72.06 $\pm$ 0.392
pH 7.4 Phosphate Buffer	26	72.61	72.30	72.92	72.61 $\pm$ 0.310
pH 7.4 Phosphate Buffer	28	73.15	72.84	73.39	73.13 $\pm$ 0.272
pH 7.4 Phosphate Buffer	30	73.62	73.16	73.92	73.57 $\pm$ 0.386

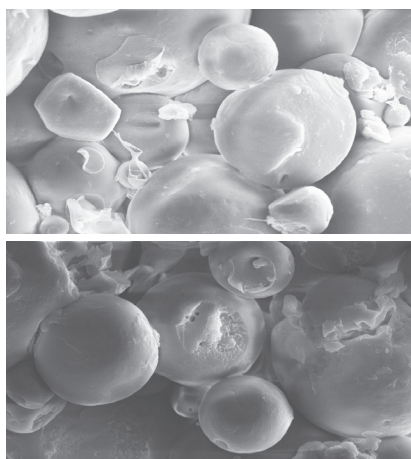


Figure 8: SEM images of valganciclovir loaded optimized formulation

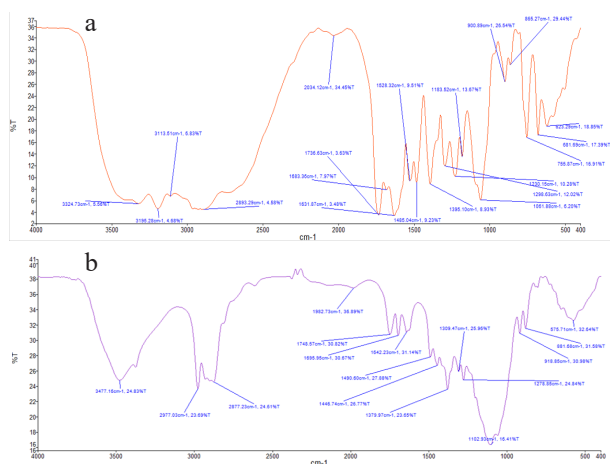


Figure 9: (a) FTIR spectra of pure drug (b) FTIR spectra of optimized formulation

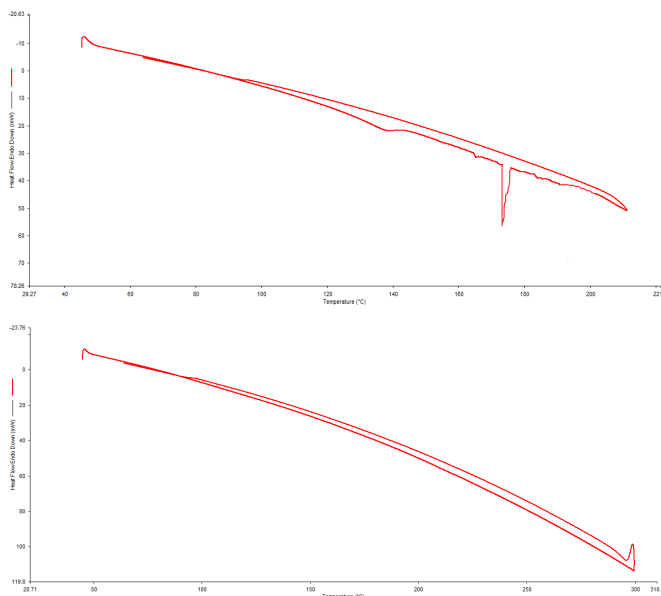


Figure 10: (a) Differential scanning calorimetry thermograms of the pure medication (b) Valganciclovir loaded nanosponges

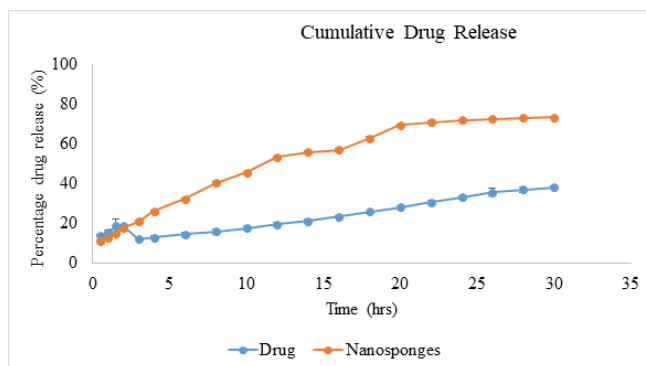


Figure 11: Cumulative drug release

Differential Scanning Calorimetry Analysis

A DSC thermogram of pure medication VGC and an optimized formulation are shown in Figures 10 (a) and (b). The prominent endothermic peak of VGC is present at 171°C in Figure 10 (a), indicating the melting point of the drug. In Figure 10 (b), the peak is not visible which might be due to encapsulation of VGC in NS.

In-vitro Drug Release

Drug release in a controlled laboratory environment for both pure drug and optimized formulation is presented in Tables 7 and 8, respectively. The total amount of drug released over time is illustrated in Figure 11. The dissolution investigation of the pure medication and formulation F8 was conducted in 0.1N hydrochloric acid for a period of 2 hours, trailed by testing in a 7.4 phosphate buffer solution.

From Figure 11 it can be clearly explained that the drug-loaded NS showed a better drug release when compared with the pure drug VGC (38.24 ± 0.452), thereby it can be concluded that VGC shows a better drug release that is 73.57% ± 0.386 when entrapped in the form of NS.

CONCLUSION

The claims made in the present research work are based on the various in-vitro trials of the formulations. The current studies conclude that the bioavailability and permeability of BCS class III drugs can be improved by using NS as a suitable carrier, decreasing dosage, and reducing side effects related to dose after in-vivo studies. In the present studies, NS was formulated using the solvent diffusion method by utilizing 3<sup>2</sup> full factorial designs for optimization of the formulation. The optimized formulation displayed a particle size of 119.1 nm, 83.61% entrapment efficiency, and -17.6 mV zeta potential. The F8 formulation showed 73.57% drug release up to 30 hours, which shows the sustained effect of the drug and proved to be a better treatment for cytomegalovirus infections.

REFERENCES

1. Taylor GH. Cytomegalovirus. Am Fam Physician. 2003 Feb 1;67(3):519-24.
2. Griffiths PD. Cytomegalovirus. Princ Pract Clin Virol. 1999 Oct 28:79-115. doi: 10.1002/0470842474.ch2c.
3. Pescovitz MD. Valganciclovir. Transplant Rev. 2006 Apr 1;20(2):82-7. doi: 10.1016/j.trre.2006.05.003.

4. Kimberlin DW, Jester PM, Sánchez PJ, Ahmed A, Arav-Boger R, Michaels MG et al. Valganciclovir for symptomatic congenital cytomegalovirus disease. *N Engl J Med*. 2015 Mar 5;372(10):933-43. doi: 10.1056/NEJMoa1404599.
5. Singh A, Chauhan CS. Nanosponges: blooming ndds in the future perspective. *Int J Pharm Sci Rev Res*. 2021;70(2):213-6. doi: 10.47583/ijpsrr.2021.v70i02.026.
6. Zainuddin R, Zaheer Z, Sangshetti JN, Momin M. Enhancement of oral bioavailability of anti-HIV drug rilpivirine HCl through nanosponge formulation. *Drug Dev Ind Pharm*. 2017 Dec 2;43(12):2076-84. doi: 10.1080/03639045.2017.1371732.
7. Rao MRP, Chaudhari J, Trotta F, Caldera F. Investigation of cyclodextrin-based nanosponges for solubility and bioavailability enhancement of rilpivirine. *AAPS PharmSciTech*. 2018 Jul;19(5):2358-69. doi: 10.1208/s12249-018-1064-6.
8. Gohel M, Patel M, Amin A, Agrawal R, Dave R, Bariya N. Formulation design and optimization of mouth dissolve tablets of nimesulide using vacuum drying technique. *AAPS PharmSciTech*. 2004 Sep;5(3):e36. doi: 10.1208/pt050336.
9. Sri KV, Santhoshini G, Sankar DR, Niharika K. Formulation and evaluation of rutin loaded nanosponges. *Asian J Res Pharm Sci*. 2018;8(1):21-4. doi: 10.5958/2231-5659.2018.00005.X.
10. Penjuri SCB, Ravouru N, Damineni S, Bns S, Poreddy SR. Formulation and Evaluation of Lansoprazole Loaded Nanosponges. *Turk J Pharm Sci*. 2016 Sep 1;13(3):304-10. doi: 10.4274/tjps.2016.04.
11. Alka S. Development and evaluation of cyclodextrin based nanosponges for bioavailability enhancement of poorly bioavailable drug. *World J Pharm Pharm Sci*. 2017;6:805-36.
12. Pandya KD, Shah NV, Gohil DY, Seth AK, Aundhia CJ, Patel SS. Development of risedronate sodium-loaded nanosponges by experimental design: optimization and in vitro characterization. *Indian J Pharm Sci*. 2019 Mar 1;81(2). doi: 10.36468/pharmaceutical-sciences.512.
13. Moin A, Roohi NKF, Rizvi SMD, Ashraf SA, Siddiqui AJ, Patel M et al. Design and formulation of polymeric nanosponge tablets with enhanced solubility for combination therapy. *RSC Adv*. 2020;10(57):34869-84. doi: 10.1039/d0ra06611g.
14. Pawar S, Shende P. Design and optimization of cyclodextrin-based nanosponges of antimalarials using central composite design for dry suspension. *J Inclusion Phenom Macrocyclic Chem*. 2021 Apr;99(3-4):169-83. doi: 10.1007/s10847-020-01038-2.
15. Rashid AE, Ahmed ME, Hamid MK. Evaluation of Antibacterial and Cytotoxicity Properties of Zinc Oxide Nanosponges Synthesized by Precipitation Method against Methicillin-resistant *Staphylococcus aureus*. *International Journal of Drug Delivery Technology*. 2022, 12(3), 985-989. DOI: 10.25258/ijddt.12.3.11
16. Issa AA, Maraie NK. Fabrication and Optimization of Prolonged-release Microcapsules Containing Protein Drug (Erythropoietin). *International Journal of Drug Delivery Technology*. 2022;12(2):564-572. DOI: 10.25258/ijddt.12.2.17
17. Khan FN, Baig MS, Nihalani G, Anees MI, Deshingkar NV. Formulation of Generic Atorvastatin Calcium Tablet by Reverse Engineering Technique. *International Journal of Pharmaceutical Quality Assurance*. 2021;12(2):14-20. DOI: 10.25258/ijpqa.12.2.03
18. Sriram P, Arsham P, Thout Reddy R, Suttee A. Formulation and evaluation of levocetirizine dihydrochloride and ambroxol hydrochloride lozenges. *International Journal of Pharmaceutical Quality Assurance*. 2020;11(3):417-423.
19. Aarti N, Ravindra K. Formulation and Evaluation of Fenofibrate Dry Emulsion Tablets by Freeze Drying Method. *International Journal of Pharmaceutical Quality Assurance*. 2022;13(4):369-376. DOI: 10.25258/ijpqa.13.4.05.